



Pro-inflammatory T helper 17 directly harms oligodendrocytes in neuroinflammation

Catherine Larochelle^{a,b,1,2}, Beatrice Wasser^{a,1}, H  l  ne Jamann^{b,1}, Julian T. L  ffel^a, Qiao-Ling Cui^c, Olivier Tastet^b, Miriam Schillner^a, Dirk Luchtman^a, J  r  me Birkenstock^a, Albrecht Stroh^d, Jack Antel^c, Stefan Bittner^{a,1}, and Frauke Zipp^{a,1,2}

^aDepartment of Neurology, Focus Program Translational Neuroscience (FTN) and Immunotherapy (FZI), Rhine-Main Neuroscience Network, University Medical Center of the Johannes Gutenberg University Mainz, 55131 Mainz, Germany; ^bCentre de Recherche du Centre Hospitalier de l'Universit   de Montr  al, Department of Neurosciences, Montreal, QC H2X 0A9, Canada; ^cMontreal Neurological Institute, Department of Neurology and Neurosurgery, McGill University, Montreal, QC H3A 2B4, Canada; and ^dInstitute for Pathophysiology, Focus Program Translational Neuroscience (FTN), University Medical Center of the Johannes Gutenberg University Mainz, 55128 Mainz, Germany

Edited by Lawrence Steinman, Stanford University School of Medicine, Stanford, CA, and approved June 14, 2021 (received for review December 29, 2020)

T helper (Th)17 cells are considered to contribute to inflammatory mechanisms in diseases such as multiple sclerosis (MS). However, the discussion persists regarding their true role in patients. Here, we visualized central nervous system (CNS) inflammatory processes in models of MS live in vivo and in MS brains and discovered that CNS-infiltrating Th17 cells form prolonged stable contact with oligodendrocytes. Strikingly, compared to Th2 cells, direct contact with Th17 worsened experimental demyelination, caused damage to human oligodendrocyte processes, and increased cell death. Importantly, we found that in comparison to Th2 cells, both human and murine Th17 cells express higher levels of the integrin CD29, which is linked to glutamate release pathways. Of note, contact of human Th17 cells with oligodendrocytes triggered release of glutamate, which induced cell stress and changes in biosynthesis of cholesterol and lipids, as revealed by single-cell RNA-sequencing analysis. Finally, exposure to glutamate decreased myelination, whereas blockade of CD29 preserved oligodendrocyte processes from Th17-mediated injury. Our data provide evidence for the direct and deleterious attack of Th17 cells on the myelin compartment and show the potential for therapeutic opportunities in MS.

oligodendrocytes | intravital microscopy | Th17 cells | glutamate | CD29 blockade

Multiple sclerosis (MS) is a disabling inflammatory disease of the central nervous system (CNS) characterized by demyelination as a key pathological hallmark (1). Loss of metabolic support and axonal myelination provided by oligodendrocytes not only impairs neurotransmission but also compromises neuronal homeostasis, leading to neuroaxonal vulnerability (2, 3). Chronic demyelination is therefore considered to play a major role in the progression of neurological disability in MS (4–6). The pharmacological protection of oligodendrocytes has been discussed as a new therapeutic strategy for MS (7) and is especially appealing in light of recent results showing that oligodendrocyte damage is partially reversible (8). However, the mechanisms underlying immune-mediated oligodendrocyte injury in neuroinflammation are still only partially understood.

Proinflammatory CD4⁺ T cells are considered to play a major role in neuroinflammatory processes in MS and in its animal model, experimental autoimmune encephalomyelitis (EAE) (9–11). In particular, interleukin (IL)-23-polarized T helper (Th)17 cells coexpressing T-bet and ROR-  are considered pathogenic in both EAE (12, 13) and in MS (13–15). Interestingly, in MS subjects, reduced Th17 responses after hematopoietic stem cell transplantation (16) or the exclusion of the double-positive Th17/1 cells from the CNS compartment after treatment with natalizumab (17) is associated with a dramatic decrease in the accumulation or expansion of demyelinating lesions, while interfering with IL-17A-cytokine signaling had moderate effects on disease severity (18). The capacity of IL-23-skewed Th17 cells to destabilize the

blood–brain barrier (BBB) and recruit antigen-presenting cells to the CNS compartment in neuroinflammation is well established (13, 19, 20), but it is not clear whether Th17 cells cause tissue injury themselves. Previous studies have demonstrated that activated CD4⁺ T cells can exert cytotoxicity toward human and rodent oligodendrocytes (21–23) in vitro and impair remyelination in a toxic mouse model (24). Of note, older in vitro reports, from prior to the discovery of Th17 cells, using human oligodendrocytic cell lines rather excluded a soluble cytokine mediator of adult oligodendrocyte lysis (21, 25). Therefore, our goal was to unravel the direct influence of Th17 cells on the myelin compartment in neuroinflammation.

Results

Direct Contact between CD4⁺ Th17 Cells and Oligodendrocytes In Vivo in EAE. To assess whether disease-inducing Th17 cells attack oligodendrocytes in vivo, we used intravital two-photon laser scanning microscopy in the upper brain stem, an area prone to active inflammation in EAE (26, 27). To visualize the dynamic interactions of both cell types in neuroinflammation, we induced

Significance

Multiple sclerosis (MS) is a neuroinflammatory, demyelinating disease that represents one of the most frequent causes of irreversible disability in young adults. Treatment options to halt disability are limited. We discovered that T helper (Th)17 cells in contact with oligodendrocytes produce higher levels of glutamate and induce significantly greater oligodendrocyte damage than their Th2 counterpart. Blockade of CD29, which is linked to glutamate release pathways and expressed in high levels on Th17 cells, preserved human oligodendrocyte processes from Th17-mediated injury. Our data thus provide evidence for the direct and deleterious attack of Th17 cells on the myelin compartment and show the potential for therapeutic opportunities to protect oligodendrocytes' myelinating processes in MS.

Author contributions: C.L., B.W., H.J., S.B., and F.Z. designed research; C.L., B.W., H.J., J.T.L., Q.-L.C., O.T., M.S., D.L., J.B., A.S., and J.A. performed research; C.L., B.W., H.J., J.T.L., Q.-L.C., O.T., D.L., J.B., A.S., J.A., S.B., and F.Z. analyzed data; and C.L., B.W., H.J., S.B., and F.Z. wrote the paper.

The authors declare no competing interest.

This article is a PNAS Direct Submission.

This open access article is distributed under [Creative Commons Attribution-NonCommercial-NoDerivatives License 4.0 \(CC BY-NC-ND\)](https://creativecommons.org/licenses/by-nc-nd/4.0/).

¹C.L., B.W., H.J., S.B., and F.Z. contributed equally to this work.

²To whom correspondence may be addressed. Email: zipp@uni-mainz.de or catherine.larochelle.chum@ssss.gouv.qc.ca.

This article contains supporting information online at <https://www.pnas.org/lookup/suppl/doi:10.1073/pnas.2025813118/-DCSupplemental>.

Published August 20, 2021.

EAE by transfer of fluorescent autoreactive IL-23-skewed Th17 cells and myelin oligodendrocyte glycoprotein (MOG)-reactivated green (GFP⁺) or cyan (CFP⁺) fluorescent protein CD4⁺ T cells isolated from actively immunized 2D2 T cell receptor (TCR) transgenic mice or C57BL/6 mice into C57BL/6-CNP-Cre × C57BL/6.1oxp.ROSA.tdRFP (CNP^{tdRFP}) recipient mice, in which oligodendrocytes express red fluorescent protein (RFP). We observed that infiltrating pathogenic Th17 cells interact with oligodendrocytes in acute EAE mice imaged 2 to 3 d after symptom onset (Fig. 1). In-depth analysis of direct visualization of the cells (Fig. 1A), as well as analysis of the surface reconstructed images (Fig. 1B and C) using three-dimensional (3D) rotation and 3D slice view to verify contacts, revealed stable long-lasting contacts between oligodendrocytes and T cells for up to 73 min (Fig. 1A–D). Interestingly, 40% of all T cell–oligodendrocyte interactions lasted longer than 5 min and 23% longer than 10 min (Fig. 1D). We further observed that, while T cells engaging in contacts lasting more than 10 min often contacted only one or two oligodendrocytes during the observation period, other T cells contacted various oligodendrocytes and showed up to 12 contacts with different oligodendrocyte areas (Fig. 1C and E), exhibiting a scanning

behavior. Based on these observations and knowledge from *in vivo* functional cellular interactions in other organs (28, 29), stable contacts were defined as those lasting at least 10 min, while scanning behavior was defined to represent T cells exhibiting multiple short contacts, with at least one contact lasting for more than 5 min. More than 40% of T cells showed a scanning behavior, and more than 30% engaged in stable interactions (Fig. 1F). Representative T cell tracks (mean track velocity) for the two behavior types “scanning behavior” and “stable contacts” are shown in Fig. 1G. Notably, Th17 cells exhibiting a scanning behavior significantly reduced their migratory speed and meandering index compared to noninteracting cells (no contact of more than 5 min). This effect was even more pronounced in cells displaying stable interactions, which showed a significantly lower migratory speed and meandering index and a higher arrest coefficient than both scanning and noninteracting cells (Fig. 1H). Altered T cell motility after engagement in long contacts with oligodendrocytes within the CNS indicates a functional interaction between oligodendrocytes and T cells. To exclude mouse strain-specific artifacts, fluorescent MOG-reactivated IL-23-skewed CD4⁺ T cells from 2D2 and C57BL/6 mice transferred into CNP^{tdRFP} were analyzed separately,

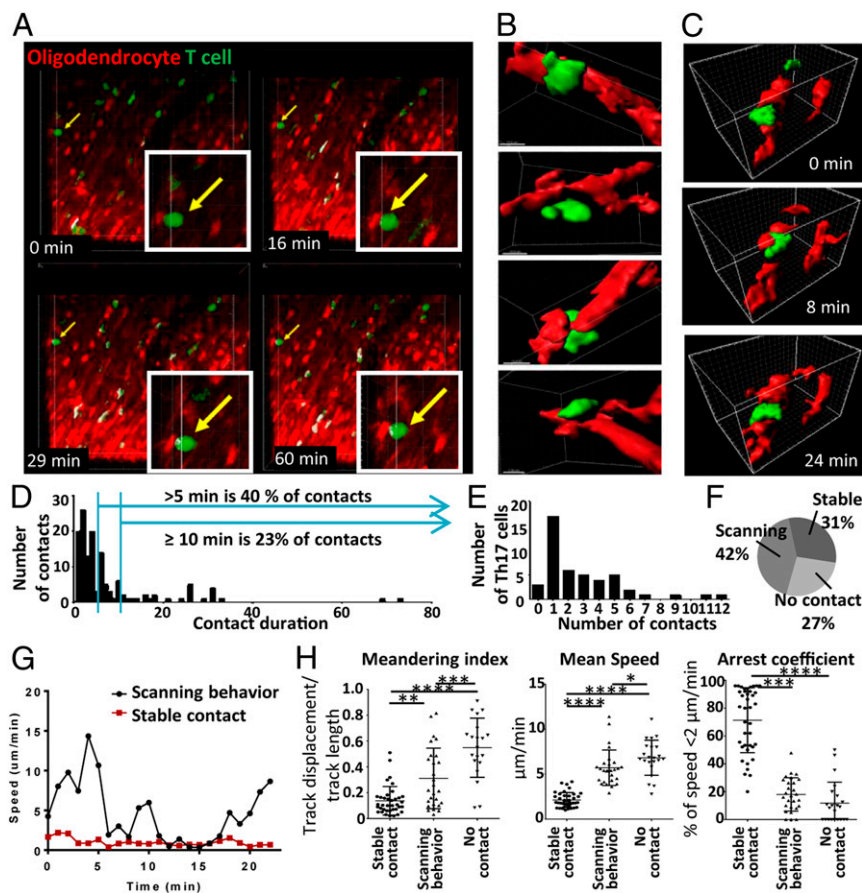


Fig. 1. CD4⁺ Th17 cells directly contact oligodendrocytes in EAE. EAE was induced in C57BL/6-CNP-Cre × C57BL/6.1oxp.ROSA.tdRFP (CNP^{tdRFP}) recipient mice by the transfer of fluorescent myelin-reactivated Th17-skewed cells (C57BL/6 or 2D2 GFP or CFP cells). *In vivo* two-photon laser scanning microscopy was performed in the upper brainstem 2 to 3 d after EAE symptom onset (score around 2.0 to 2.5). (A) Visualization of oligodendrocytes (red) and T cells (green) over a period of 60 min. (B) Visualization of surface reconstructed images of an oligodendrocyte (red)–T cell (green) interaction from four different angles. (Scale bar, 10 μm.) (C) Visualization of surface reconstructed images of a T cell (green) interacting with different oligodendrocyte (red) areas. (D) Quantification of the contact duration between T cells and oligodendrocytes. *n* = 49 cells from four different mice, one movie per mouse. Blue vertical lines mark 5 min and 10 min contact duration; horizontal arrows represent the range of duration of contact beginning with 5 or 10 min. (E) Quantification of the number of distinct oligodendrocyte areas a T cell is interacting with in a period of up to 73 min. *n* = 49 cells from four different mice, one movie per mouse. (F) Quantification of T cell interaction types. (G) Representative examples of T cell tracks (mean track velocity) for a stable contact and a scanning behavior over time. (H) Comparison of meandering index, mean speed, and arrest coefficient between T cells showing no significant contact, scanning behavior including long-lasting (>5 min) contacts, and stable contacts (≥10 min). *n* = 88 cells from seven different mice, one movie per mouse. Statistical analysis for H was performed using one-way ANOVA with Tukey’s post hoc test. **P* < 0.05; ***P* < 0.01; ****P* < 0.001; *****P* < 0.0001.

and MOG₃₅₋₅₅ peptide-specific IL-23-skewed cells (2D2-GFP or 2D2-CFP) were transferred into *Rag2^{-/-}cgn^{-/-}* mice, in which visualization of myelin was enabled via Nile Red application. Analysis of T cell contacts with oligodendrocytes after EAE onset revealed similar results across the different strains of donor or recipient mice (SI Appendix, Fig. S1).

Oligodendrocytes were, so far, not considered to be the direct target of Th17 cells because major histocompatibility complex class II (MHC-II) is not or is only weakly expressed on oligodendrocytes (30–32). We next aimed to analyze whether T cell–oligodendrocyte interactions were dependent on an unforeseen up-regulation of MHC-II molecules on oligodendrocytes in the CNS of EAE mice. Using immunofluorescence, we identified both oligodendrocytes and MHC-II-expressing cells in EAE lesions but no coexpression of MHC-II and the oligodendrocytic marker Nogo-A (Fig. 2A). Analysis of T cell–oligodendrocyte interactions via immunofluorescence further showed the absence of MHC-II expression at the site of T cell–oligodendrocyte direct interaction, showing that T cell–oligodendrocyte close contacts are not restricted by the need for expression of MHC-II (Fig. 2B). Next, we cotransferred polyclonal Th17 cells (IL-23-skewed

B6.GFP cells activated with anti-CD3/anti-CD28 in vitro) with MOG-specific Th17 cells (IL-23-skewed B6.2D2.CFP cells activated with anti-CD3/anti-CD28 in vitro) into *Rag2^{-/-}cgn^{-/-}* mice in order to induce EAE in these mice and take advantage of the BBB dysfunction to allow for infiltration of polyclonal Th17 cells into the CNS of the diseased mice (SI Appendix, Fig. S2A). We found that not only MOG-specific Th17 cells but also polyclonal Th17 cells could form prolonged stable interactions with oligodendrocytes in vivo (Fig. 2C–E). Although the mean track velocity was significantly higher and the arrest coefficient lower in polyclonal Th17 cells (SI Appendix, Fig. S2B), the amount of stable contacts and the scanning behavior did not differ significantly between myelin-specific and polyclonal Th17 cell populations (Fig. 2E). The polyclonal repertoire of B6.GFP mice contains a small fraction of MOG-specific CD4, which can become enriched in the CNS during EAE. Therefore, due to a higher capacity of MOG-specific T cells to infiltrate the CNS compared to non-antigen-specific T cells (33), we additionally analyzed interactions of MOG-specific T cells and OT-II-specific T cells with oligodendrocytes in organotypic hippocampal slice cultures. In this model, interactions of MOG-specific T cells can

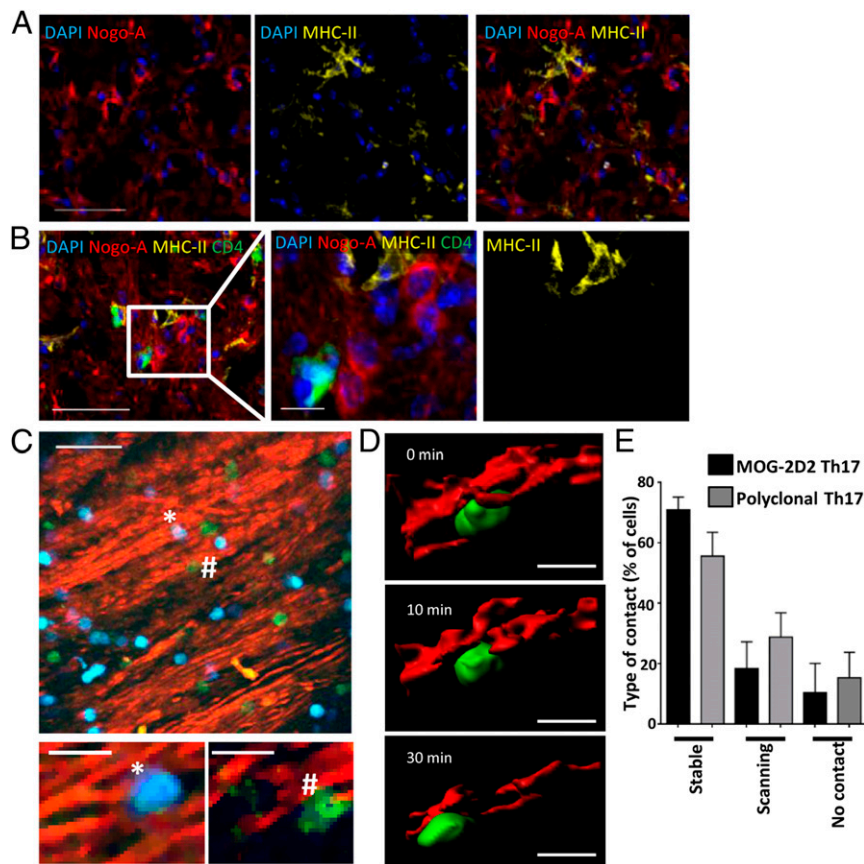


Fig. 2. Interactions of T cells and oligodendrocytes are not limited to MOG-specific T cells. EAE was induced in *Rag2^{-/-}cgn^{-/-}* recipient mice by the transfer of Th17-skewed cells. Immunofluorescence was performed in the brain stem in EAE lesions. (A) Immunofluorescence costainings of Nogo-A (red, oligodendrocytes) with DAPI (blue, cell nuclei) (Left), MHC-II (yellow) with DAPI (Middle), and the overlay of Nogo-A, MHC-II, and DAPI (Right). Representative of a total of 17 different regions from eight distinct brain stem sections derived from two EAE mice (score of 2.0). (Scale bar, 50 μ m.) (B) Immunofluorescence staining of Nogo-A (red), MHC-II (yellow), CD4 (T cells, green), and nucleus (DAPI, blue). Shown is a representative overview of the interactions of oligodendrocytes and T cells in an EAE lesion (Left) and a magnified view of a T cell–oligodendrocyte interaction (Right). (Scale bars, 50 and 10 μ m.) (C–E) In vivo two-photon laser scanning microscopy was performed in the upper brain stem at the onset of EAE disease. (C) Visualization of oligodendrocytes (red), 2D2 T cells (blue), and polyclonal CD4+ T cells (green) (Upper) and magnification of representative interactions between an oligodendrocyte and each of these T cell types (Lower). (Scale bars, 40 and 10 μ m.) (D) Visualization of surface-reconstructed images of an interaction between an oligodendrocyte (red) with a polyclonal CD4+ T cell (green) over a period of 30 min. (Scale bar, 10 μ m.) (E) Comparison of interaction types between oligodendrocytes and either polyclonal or MOG-specific (2D2) CD4+ T cells. $n = 48$ MOG-specific 2D2 cells and $n = 44$ polyclonal T cells from three different mice, one movie per mouse. Statistical analysis was performed using two-tailed unpaired *t* test.

be analyzed directly in comparison to T cells, which are specific to the non-CNS antigen ovalbumin. Again, we observed no differences in the amount of stable contacts and scanning behavior (*SI Appendix, Fig. S2C*). Taken together, these findings indicate that interactions with oligodendrocytes are not limited to antigen-specific Th17 cells.

Local Harmful Interaction between Effector and Target Cells Not Only in EAE but Also in MS. To determine if the observed CD4⁺ T cell–oligodendrocyte interactions could be relevant to human MS pathobiology, we next aimed to analyze whether CD4⁺ T cells contact oligodendrocytes in the CNS of EAE mice and of MS subjects. Using immunofluorescence studies, we found that in both passive transfer EAE and in active EAE, over 10% of CD4⁺ T cells present in the CNS tissue (spinal cord and brain stem) are in close contact with oligodendrocytes (Fig. 3*A* and *B*). Importantly, on fresh-frozen postmortem brain sections from the CNS of MS subjects, we were able to show in situ CD4⁺ T cells in direct juxtaposition with oligodendrocytes both in the white matter (WM) parenchyma next to perivascular cuffs of immune cells typical for MS lesions (perilesional WM) and in the normal-appearing WM (NAWM) (Fig. 3*C* and *D*). Analyzing images

using 1- μ m z-slices (from 8- μ m z-stacks), we further found that around 15 to 30% of the observed CD4⁺ T cells infiltrating the WM parenchyma in MS brains are in contact with an oligodendrocyte (Fig. 3*E*). This data suggests that direct contacts between CNS-infiltrating CD4⁺ T cells and oligodendrocytes, as we observed in vivo and in situ in different EAE models, are also present in human MS.

To assess the impact on oligodendrocytes of direct interaction with CD4 T cells, we first performed immunofluorescence studies on the CNS of symptomatic EAE mice (clinical score of 2.0 to 3.0). A significantly higher percentage of oligodendrocytes exhibited caspase activity when the oligodendrocyte cell bodies were in close proximity to T cells compared to oligodendrocytes without contact with T cells both in passive and active EAE (*SI Appendix, Fig. S3 A and B*), indicating probable T cell cytotoxicity toward oligodendrocytes in vivo.

Next, to examine the specific impact of pathogenic IL-23-skewed Th17 cells on oligodendrocytes and demyelination/remyelination in a dynamic system (13), we compared the impact of IL-23-skewed Th17 cells to that of IL-4-skewed Th2 cells, which are considered beneficial in MS and EAE (34, 35). We used an organotypic hippocampal slice model to circumvent the low capacity of Th2

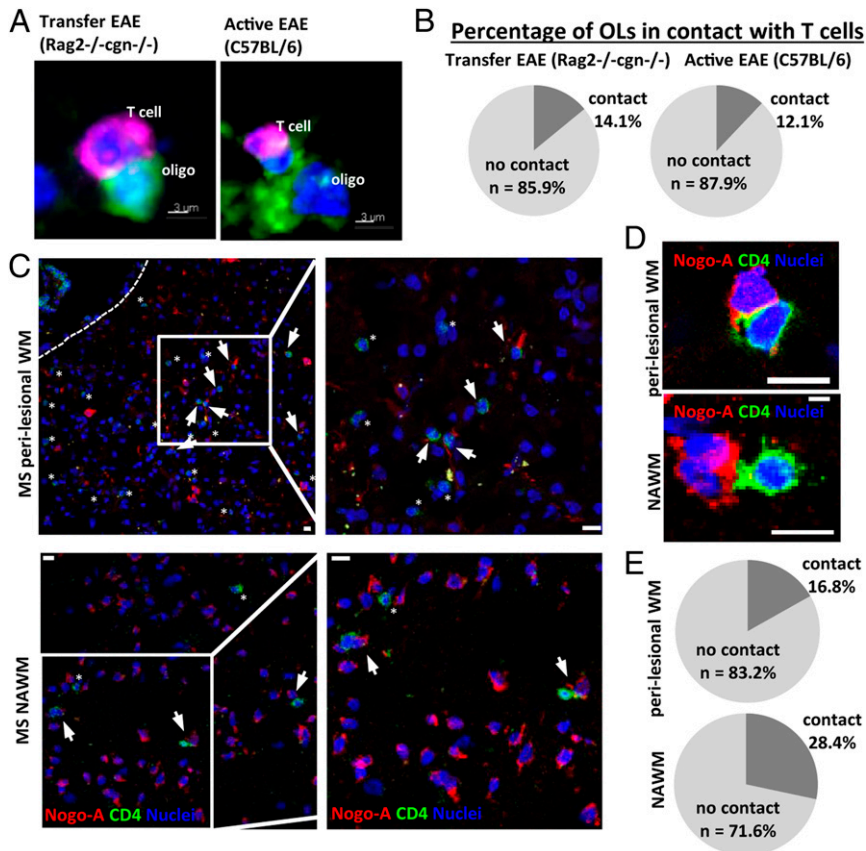


Fig. 3. CD4⁺ T cells form contacts with oligodendrocytes in the CNS of active and passive EAE mice and of human MS subjects. (*A* and *B*) EAE was induced in *Rag2*^{-/-}*cgn*^{-/-} recipient mice by the transfer of Th17-skewed cells or in C57BL/6 mice by active MOG₃₅₋₅₅ immunization. (*A*) Immunofluorescence was performed in EAE spinal cords to visualize Olig2 (oligodendrocytes, green), CD4 (T cell, magenta), and DAPI (blue). Representative images of T cell–oligodendrocyte interactions. (Scale bar, 3 μ m.) (*B*) Quantification of oligodendrocytes with or without current contact to T cells in C57BL/6 ($n = 7$ sections from five distinct EAE animals, clinical score 2 to 3) and *Rag2*^{-/-}*cgn*^{-/-} mice ($n = 7$ sections from five distinct EAE animals, clinical score 2 to 3). (*C–E*) Immunofluorescence staining was performed on human MS CNS postmortem material in perilesional WM and NAWM. (Scale bars, 10 μ m.) (*C*) Representative immunofluorescence stainings from postmortem CNS samples of MS subjects showing Nogo-A (oligodendrocytes, red), CD4 (T cells, green), and Topro (cell nucleus, blue) in perilesional WM (Upper) and NAWM (Lower). (Scale bar, 10 μ m.) Arrowheads mark T cells in contact with oligodendrocytes, asterisks mark T cells without contact with an oligodendrocyte. Dashed white line indicates perivascular space. (*D*) High magnification showing examples of direct contacts between CD4⁺ cells (green) and oligodendrocytes (red) in the perilesional WM (Upper) and the NAWM (Lower) in MS CNS. (*E*) Pie chart reflecting the quantification of CD4⁺ T cells in the WM parenchyma in direct juxtaposition (contact) or not (no contact) with oligodendrocytes in human MS perilesional WM (Upper) or NAWM (Lower). CD4⁺ cells located within the vessel/perivascular space were excluded from analysis.

cells to cross the BBB (36). In this model, murine hippocampal slices show extensive myelination after 10 d *in vitro*. Addition of lysophosphatidyl choline (LPC) on the myelinated slices triggers a reversible toxic myelin injury, mimicking CNS conditions in MS. In line with our *in situ* data, using this model, we could show that addition of Th17 cells worsens demyelination (Fig. 4 *A* and *B*), showing a deleterious impact of Th17 cells on myelin-producing oligodendrocytes after LPC injury *in vitro*. Interestingly, no negative impact on demyelination/remyelination processes was observed when Th2 cells were added, suggesting that the deleterious impact on oligodendrocytes is specific to proinflammatory CD4⁺ T cell subsets. To isolate the direct and specific impact of proinflammatory T cells on oligodendrocytes and parallel these results in a human setup, we exposed human adult oligodendrocytes in primary culture to either supernatant of activated human Th17-polarized cells or direct coculture with Th17-polarized or Th2-polarized activated CD4⁺ T cells. Of note, in this setup, virtually no CNS-derived cells express human leukocyte antigen (HLA)-DR and/or CD11b (routinely less than 5%), thereby excluding a major contribution of antigen-dependent mechanisms,

HLA mismatch, or indirect impact through contaminating microglial cells. With this model, we found that contact with human Th17-polarized activated CD4⁺ T cells induces a higher proportion of oligodendrocyte cell death compared to contact with Th2-polarized activated CD4⁺ T cells or Th17 cell supernatant *in vitro* (Fig. 4 *C* and *D* and *SI Appendix*, Fig. *S3 C* and *D*). Most interestingly, in line with our observations in murine organotypic slices, human Th17-polarized activated CD4⁺ T cells strikingly reduced the total area and branching level complexity of the processes of human oligodendrocytes, while Th2-polarized activated CD4⁺ T cells showed a significantly milder impact (Fig. 4 *E* and *F* and *SI Appendix*, Fig. *S3E*). Similarly, we found a significant worsening of injury to oligodendrocyte cell processes when comparing the impact of α -CD3/ α -CD28-activated CD4⁺ T cells from MS subjects with their counterpart from age- and sex-matched healthy controls (Fig. 4 *G* and *H*). Thus, these results show that Th17-polarized cells can exert significant cytotoxicity toward oligodendrocytes and, in line with previous reports (21, 25), that proinflammatory T cell-mediated oligodendrocyte injury is at least partially dependent on close cellular interactions.

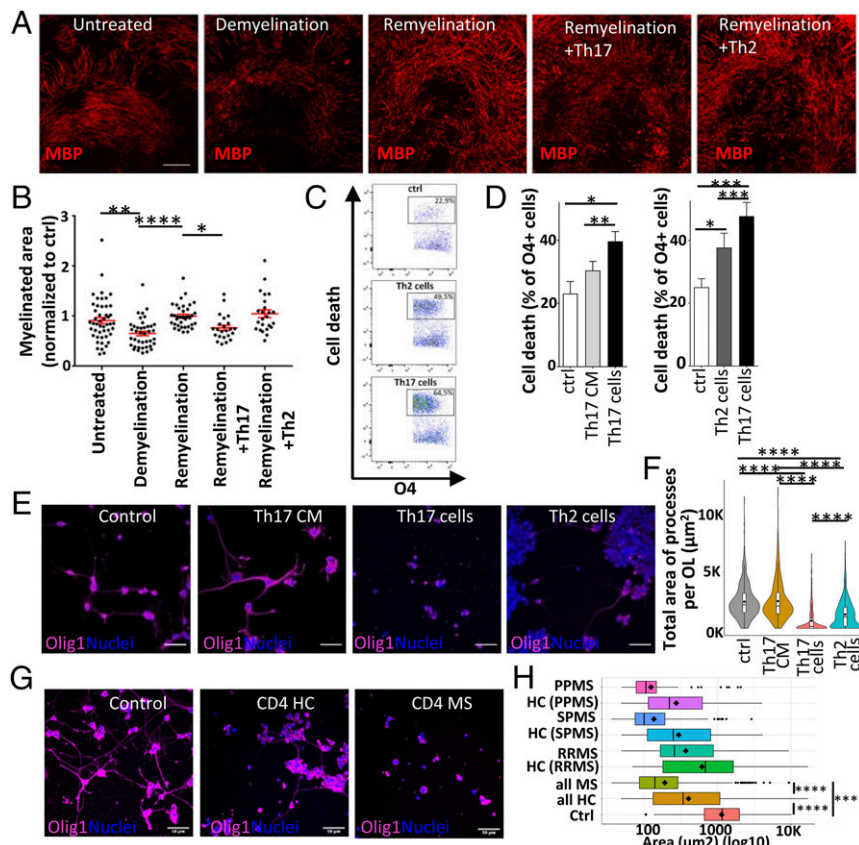


Fig. 4. T cells mediate oligodendrocyte cell injury. (*A* and *B*) Analysis of the myelinated area in organotypic hippocampal slices after LPC-induced demyelination by immunofluorescence; (*A*) representative confocal images, (*B*) quantification. The myelinated area was determined 48 h after LPC-induced demyelination (“Demyelination,” $n = 40$ reslices, day 12 of culture) or in the untreated control group (“untreated,” $n = 48$, day 12 of culture), and 10 d after LPC-induced demyelination, with or without the presence of CD4⁺ T cells (“Remyelination,” $n = 37$; “Remyelination + Th17,” $n = 23$; “Remyelination + Th2,” $n = 24$, day 20 of culture). (Scale bar, 100 μm .) (*C–H*) Analysis of human oligodendrocyte cell injury following direct exposure to human CD4⁺ T cells or exposure to T cell-conditioned medium (CM) *in vitro*. (*C*) Representative contour pseudocolor dot plots showing oligodendrocyte (OL) cell death after exposure to Th17 cells or Th2 cells. (*D*) Quantitative comparison of the capability to induce human oligodendrocyte cell death between Th17 cells, Th2 cells, and Th17-conditioned medium (Th17 CM) (Left, $n \geq 6$ T cell donors, ≥ 3 different OL preparations). (*E*) Representative confocal microscopy images and (*F*) quantitative analysis of the total area of processes per OL after exposure to Th17 CM, Th17 cells, or Th2 cells ($n = 4$ human T cell donors and $n = 2$ different OL preparations, processes of $n = 351$ to 509 OLs/condition). (Scale bar, 50 μm .) (*G*) Representative confocal microscopy images and (*H*) quantitative analysis of the total area of processes per OL after exposure to activated CD4⁺ T cells from MS subjects or age- and sex-matched controls on OL cell processes *in vitro* ($n = 4$ T cell MS donors: 1 secondary progressive MS (SPMS), 1 primary progressive MS (PPMS), 2 relapsing-remitting MS (RRMS) and $n = 4$ matched human control donors, $n = 3$ different OL preparations, analysis of processes from $n = 603$ OLs in coculture with MS T cells and $n = 608$ OLs in coculture with control T cells). (Scale bar, 50 μm .) Statistical analysis for *B* was performed using a Kruskal–Wallis test with Dunn’s multiple comparisons test and for *D*, *F*, and *H* by ANOVA with Tukey’s post hoc test. * $P < 0.05$; ** $P < 0.01$; *** $P < 0.001$; **** $P < 0.0001$.

Th17 Cells Express High Levels of CD29 and Release Glutamate in Contact with Oligodendrocytes. We next aimed to explore mechanisms underlying Th17 cell-mediated oligodendrocyte injury. We had previously shown that murine Th17 cells do not express high levels of the classical neurotoxic molecules granzyme B or Fas ligand (FasL) (37). In addition, while NKG2D has been implicated in human CD4⁺ T cell-mediated injury to oligodendrocytes (23), we did not observe significant differences in expression of NKG2D by Th17 compared to Th2 cells (*SI Appendix, Fig. S4A–C*). Glutamate is expressed by Th17 cells (27) and can reach high concentrations when released from vesicles in close vicinity to target cells (38). Our group has recently described CD29-triggered vesicular glutamate release by Th17 cells (37). As oligodendrocytes and their precursors can express several ligands for CD29 such as collagens, laminins, and CSPG4/NG2 (39–43), we therefore investigated a possible role of glutamate in direct Th17-mediated oligodendrocyte injury. We first compared expression of CD29, which is increased on CD4⁺ T cells from MS subjects compared to healthy controls (37), on human and murine Th17-polarized and Th2-polarized activated CD4⁺ T cells. Accordingly,

we found significantly higher levels of CD29 expressed on the surface of murine and human Th17-polarized cells compared to Th2-polarized cells (Fig. 5A and B), with higher levels on IL-17⁺ T cells compared to their IL-17^{neg} counterpart (*SI Appendix, Fig. S4D*). In contrast, no differences were observed when murine MOG-specific Th17 cells were compared to ovalbumin-specific Th17 cells or polyclonal Th17 cells (*SI Appendix, Fig. S4E*). We then compared the capacity for vesicular glutamate release of Th17 cells with Th2 cells by looking at VAMP2 and Vglut1 (canonically associated with vesicular glutamate release) as well as Xc⁻ (canonically associated with nonvesicular glutamate release). We found that murine Th17 cells show a significantly higher VAMP2/Xc⁻ ratio than their Th2 counterpart, while human T cells display a similar trend along with a significantly higher expression of Vglut1 by Th17-polarized cells (Fig. 5C and D and *SI Appendix, Fig. S4F and G*), indicating that vesicular glutamate-release pathways predominate in Th17 cells but not in Th2 cells. Indeed, glutamate levels were higher in cocultures of human MO3.13 oligodendrocytic cells with human Th17-polarized cells as compared to cocultures with Th2-polarized cells (Fig. 5E).

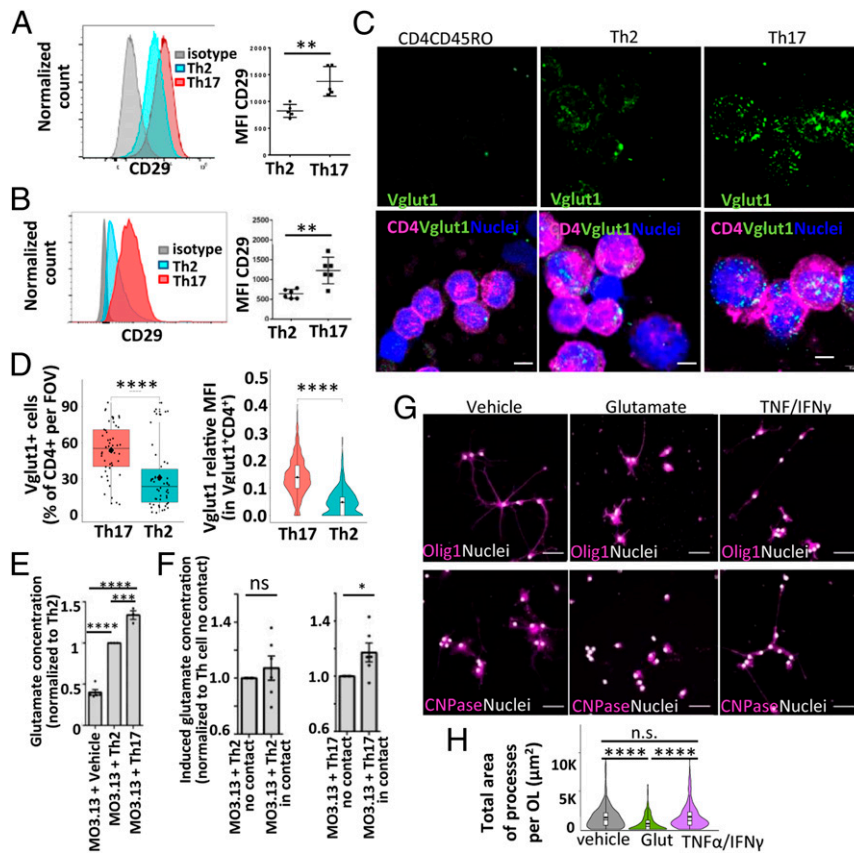


Fig. 5. Glutamate is secreted via a vesicular release pathway by Th17 but not Th2 cells and is toxic to oligodendrocyte cell processes. (A) Representative histogram (*Left*) and quantification (*Right*) of CD29 expression by median fluorescent intensity (MFI) in human Th17-polarized cells (day 6 of culture, red) and Th2-polarized cells (day 6 of culture, blue). The isotype control is shown in gray. $n = 5$ T cell donors (healthy controls). (B) Representative histogram (*Left*) and quantification of CD29 expression (*Right*) in murine Th17-skewed cells (day 5 of culture, red) and Th2-skewed cells (day 5 of culture, blue). The isotype control is shown in gray. $n = 6$ independent cultures with splenocytes from six mice. (C and D) Vglut1 expression by human Th2 and Th17 cells. (C) Representative confocal microscopy images (cytospin) of human memory CD4 T cells ex vivo (CD4CD45RO), Th2, and Th17 cells (day 6 in culture). (D) Quantitative analysis (*Left*) of number of Vglut1⁺CD4⁺ per field of view (FOV) and (*Right*) relative median intensity of Vglut1 signal on Vglut1⁺CD4⁺ cells ($n = 5$ donors, 10 FOV/condition, ≥ 15 cells/FOV). (Scale bar, 5 μm .) (E and F) Glutamate concentration was determined in cocultures of MO3.13 oligodendrocytes with Th17 cells or Th2 cells and normalized to the coculture with Th2 cells (E). (F) Induced glutamate levels (after subtraction of basal glutamate level in MO3.13 cultures and normalized to “no contact”) was compared in the direct coculture of Th2 cells (*Left*) or Th17 cells (*Right*) with MO3.13 oligodendrocytes (“in contact”) and the coculture using an insert to separate T cells from oligodendrocytes (“no contact”). (G and H) Impact of exposure to proinflammatory cytokines TNF- α and IFN- γ or to glutamate on oligodendrocyte (OL) cell processes in vitro. (G) Representative confocal microscopy images and (H) quantitative analysis of the total area of processes per OL ($n = 3$ different OL preparations, analysis of $n \geq 200$ OLs/condition). (Scale bar, 50 μm .) Statistical analyses were performed using two-sided paired (A, D, and F) and unpaired (B) Student’s *t* test or one-way ANOVA with Tukey’s post hoc test (E and H). n.s.: not significant; * $P < 0.05$; ** $P < 0.01$; *** $P < 0.001$; **** $P < 0.0001$.

Moreover, we could observe a contact-dependent induction of glutamate release in Th17/MO3.13 cocultures, which was not observed in Th2/MO3.13 cocultures (Fig. 5F). Taken together, our data indicate a higher capacity of Th17 cells compared to their Th2 counterpart for CD29-triggered release of glutamate upon contact with oligodendrocytes.

Glutamate Is Deleterious to Oligodendrocyte Processes and Impairs Myelination. As we found that Th17-polarized cells release glutamate in contact with oligodendrocytic cells, we then assessed the impact of glutamate itself on human oligodendrocytes in primary culture. We found that 12- to 24-h application of glutamate—but not proinflammatory cytokines TNF- α or IFN- γ —strongly decreased the area and complexity of human oligodendrocyte processes in vitro without affecting oligodendrocyte survival (Fig. 5G and H and *SI Appendix, Fig. S4H*). To further investigate the impact of glutamate on human oligodendrocytes, we used single-cell RNA sequencing (scRNAseq) of the human oligodendrocytes in primary culture, unstimulated (vehicle) and stimulated with glutamate (Fig. 6A and B) (44). After removing expected small populations of immune cells that did not feature transcriptional characteristics of oligodendrocytes (*SI Appendix, Fig. S5A*) and of cells expressing a high proportion of mitochondrial genes (45), five clusters of CNS-resident cells were identified by the shared nearest neighbor (SNN) clustering algorithm (Fig. 6A). Based on expression of transcription factors and of myelin-related genes (*SI Appendix, Fig. S5B*), all clusters except one (labeled EIF5+ glial cells, less than 5% of total cells) were considered to represent oligodendrocytes or oligodendrocyte progenitors (immature). Compared to the control condition, exposure to 1 mM glutamate (12 h) was associated with a slightly decreased proportion of mature oligodendrocytes (Fig. 6A), characterized by high relative expression of PLP1, CNP, MBP, and MOG (*SI Appendix, Fig. S5B*). In line with our results showing loss of CNPase⁺ oligodendrocytic cell processes upon glutamate exposure, differential expression analysis revealed that within oligodendrocyte subsets, the impact of 12 h glutamate exposure on gene expression was most pronounced on mature oligodendrocytes with 81 genes significantly altered (*SI Appendix, Fig. S5C*) and 27 of these genes above the threshold log₂ fold change (LFC) > 0.3 (Fig. 6B). Gene ontology (GO) analysis of this set of genes showed that the top regulated biological pathways in mature oligodendrocytes were related to cholesterol and lipid biosynthesis and protein translation and localization to endoplasmic reticulum (Fig. 6B and *SI Appendix, Fig. S5D and Table S1*). Among the top regulated genes were HMGCS1 and HMGCR, recently described as elevated in association with remyelination after toxic (cuprizone) myelin injury (46), that could represent a physiological response to glutamate to promote axonal ensheathing (47). However, we found that exposure to glutamate was associated with an up-regulation of INSIG1, which is a major negative regulator of cholesterol biosynthesis (48). In addition, levels of SCD-1 were increased, which promotes cell survival but interferes with cholesterol synthesis and efflux (49–51), and of TMEM97, which plays a major role in regulating cholesterol trafficking and metabolism (52) and is a target for neuroprotection (53, 54). Genes previously described as increased in oligodendrocytes from MS brains or in MS lesions compared to controls were also significantly up-regulated (ACTB, PLP1, and PTMA), as well as genes associated with oligodendrocyte differentiation and myelin biogenesis (MAL, SPP1, and TF) and with cell stress/apoptosis (PTGDS and TXNIP). Taken together, this could represent a response of oligodendrocytes to excessive glutamate stress promoting cell survival at the detriment of myelination. Notably, although not reaching significance, at this early time point, the expression of apoptosis-related TP53, XKR6, and CASP6 was elevated after glutamate exposure in the stressed oligodendrocytes cluster (*SI Appendix, Fig. S5E*). Previously, the

dysregulation of oligodendrocytic biosynthesis of cholesterol and lipids has been described as impairing myelination (46, 55, 56). In line with these results, we found that glutamate exposure impaired the ensheathing capacity of human oligodendrocytes in primary culture on nanofiber-coated microplates (Fig. 6C and D) and reduced the myelinated area in organotypic hippocampal slice cultures (Fig. 6E). These data outline the direct deleterious impact of glutamate on oligodendrocyte processes and suggest that glutamate released by Th17 cells in close contact with oligodendrocytes could contribute to oligodendrocyte cell process injury and impair myelination in inflammatory Th17-driven CNS conditions such as EAE and MS.

CD29 Blockade Protects Oligodendrocytes from Th17-Mediated Injury.

To demonstrate that human oligodendrocytes can express ligands for CD29, we assessed expression in our scRNAseq data and found that COL4A5 (collagen subunit), FN (fibronectin), and MADCAM1 show the highest messenger RNA (mRNA) expression (*SI Appendix, Fig. S6A*). We confirmed expression of these three CD29 ligands on human oligodendrocytes in primary culture at the protein level using immunofluorescence (*SI Appendix, Fig. S6B*). CD29 is heavily implicated in T cell transmigration toward the CNS compartment during EAE; CD29 genetic deletion in MOG-reactive T cells is sufficient to abrogate their capacity to invade the CNS and transfer EAE (57). Therefore, we used in vitro models to assess the specific potential of CD29 as a direct therapeutic target to protect myelinating processes from Th17-mediated injury in MS. We were able to demonstrate that pretreatment of human Th17 cells with an activating (agonistic) CD29 antibody, which is associated with glutamate release (37), significantly worsened T cell-mediated injury when MO3.13 human oligodendrocytic cell lines, which are not as susceptible to Th17-mediated injury (58), were used as target cells (Fig. 7A–C). Notably, CD29 blocking antibody ameliorated T cell-mediated injury (Fig. 7A–C). Importantly, using human oligodendrocytes in primary culture, we were able to confirm that CD29 neutralization on Th17-polarized cells before 12 h coculture is protective, while CD29 activation showed a trend of increased Th17 cell toxicity toward oligodendrocyte cell processes and decreased the number of remaining oligodendrocytes (Fig. 7D and E and *SI Appendix, Fig. S6C and D*). We had previously demonstrated that restricting glutaminase in the CNS compartment or interfering with the CD29-triggered glutamate release cascade in Th17 cells improved EAE and decreased T cell arrest in the CNS (37). Taken together with our data demonstrating preservation of oligodendrocyte processes from T cell-mediated injury upon neutralization of CD29 on Th17 cells, this suggests that CD29-triggered glutamate release by Th17 cells contributes to pathological mechanisms underlying demyelination and remyelination failure in MS (*SI Appendix, Fig. S7*).

Discussion

Although it is widely accepted that proinflammatory CD4⁺ T cells play a pivotal role in MS and EAE (59–61) and that oligodendrocyte injury contributes to the pathogenesis of both diseases (7), the processes leading to oligodendrocyte and myelin injury in inflammation are far from being understood, and therapeutic strategies protecting the myelin compartment and promoting remyelination have been so far unsuccessful. Here, we were able to show that pathogenic Th17 cells directly interact with oligodendrocytes in vivo, are detrimental to oligodendrocytes when in close contact, and can release glutamate, which impairs myelinating processes of human and murine oligodendrocytes. Importantly, we identified local CD29 modulation as a potential target to protect human oligodendrocytes against Th17 cell-mediated injury.

Using intravital microscopy, we found that 40% of all T cell–oligodendrocyte interactions occurring in the CNS of experimental neuroinflammation lasted longer than 5 min, a period of

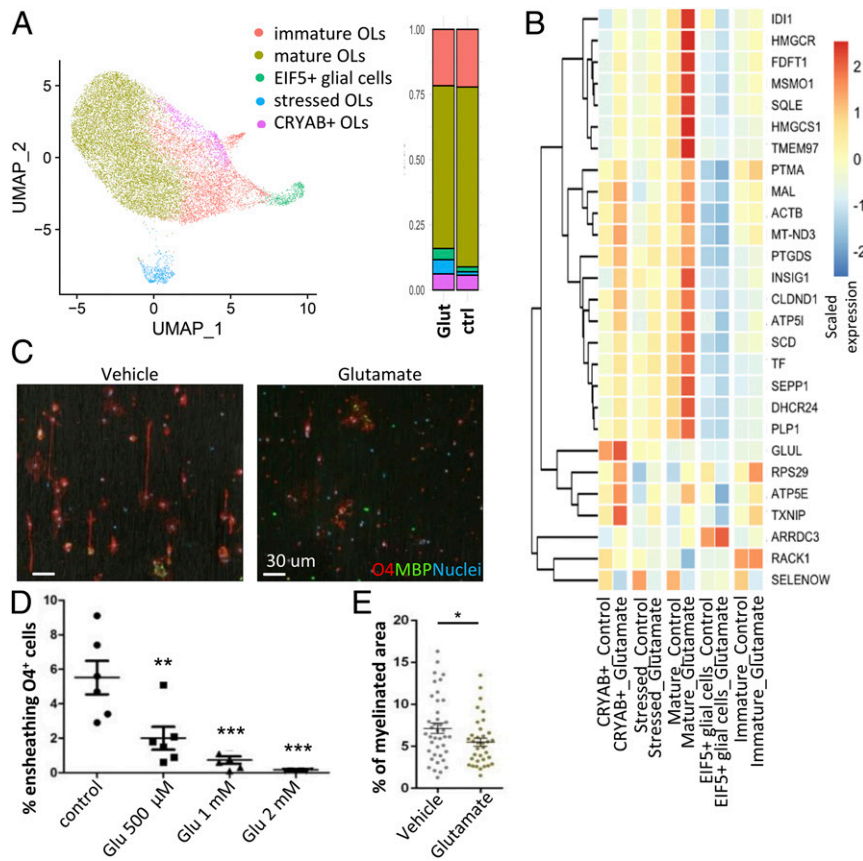


Fig. 6. Glutamate alters cholesterol biosynthesis in mature oligodendrocytes (OLs) and impairs myelination. (A and B) scRNAseq of human OLs in primary culture exposed to glutamate 1 mM or vehicle (control) for 12 h ($n = 2$ different donors/batch). (A) UMAP (uniform manifold approximation and projection) showing the results of SNN clustering and bar chart illustrating the proportion of each cluster across the different conditions (glutamate versus control). (B) Heatmap of top DEGs in mature OLs exposed to glutamate compared to control condition (adjusted P value < 0.01 , absolute LFC ≥ 0.3), relative expression scaled by gene across subpopulations and conditions (row). (C and D) Impact of glutamate on human OLs ensheathing ability on nanofibers. (C) Representative confocal microscopy images (Scale bar, 30 μm .) and (D) quantitative analysis of ensheathing OLs (each dot represents the percentage of OLs ensheathing nanofibers in one well, $n = 3$ preparations, in duplicates). (E) Impact of exposure to glutamate (1 mM) on myelinated area in organotypic hippocampal slices by immunofluorescence ($n = 40$ reslices treated with glutamate, $n = 35$ reslices for control). Statistical analysis for D was performed using one-way ANOVA with Tukey's post hoc test and for E using two-sided paired Student's t test. * $P < 0.05$; ** $P < 0.01$; *** $P < 0.001$.

time that is known to be relevant and sufficient for initiating signaling pathways in immune interactions (28, 62, 63). We previously reported that contact of 5 min duration between CD4^+ T cells and neurons is sufficient to induce intracellular calcium influx (27). Furthermore, significant biological interactions, such as T cell activation by dendritic cells, are accompanied by reduced T cell motility (28). In line with this, we observed reduced T cell motility for T cells interacting both stably and in a scanning behavior with oligodendrocytes. T cells that made contact with oligodendrocytes not only showed decreased velocity but lower meandering index and higher coefficient arrest, suggesting that these T cells spent more time interacting with oligodendrocytes than with other CNS targets, as the T cell velocity of non-interacting cells was significantly higher.

Reduced T cell motility was previously associated with antigen-dependent interactions (28). Antigen recognition is, however, not the only process affecting T cell motility, but it can be further influenced by chemokine receptors (64) and adhesion molecules (65). Importantly, we demonstrated that most oligodendrocytes do not express MHC-II at the protein level in neuroinflammatory conditions, in line with previous in vitro and in situ observations (31, 32, 66). Moreover, our human coculture setup precluded a major contribution of nonoligodendrocytic glial cells expressing significant levels of MHC-II or of indirect cytotoxicity such as through microglial activation by T cells. Despite the absence of

MHC-II on target cells, we found that close contact with Th17 cells is associated with a significant increase in damage to human oligodendrocyte cell processes compared to Th17-conditioned medium.

Comparing the prototypic pathogenic Th17 cell subset versus the prototypic anti-inflammatory and proneuroregenerative Th2 cell subset (35), we were able to demonstrate that human and murine Th17-polarized cells significantly worsen demyelination and cause severe injury to oligodendrocyte processes. Th17-polarized cells did not express higher levels of previously described neurotoxic molecules such as NKG2D when compared to their Th2-polarized counterpart, suggesting that other mechanisms underlie the observed greater Th17-mediated oligodendrocyte cell injury. In line with previous literature reporting that mature human oligodendrocytes are resistant to inflammatory cell-conditioned medium (67) and that the proinflammatory cytokines $\text{TNF-}\alpha$ and $\text{IFN-}\gamma$ are not essential to mediate inflammatory demyelination (21, 68, 69), we did not observe an increase in oligodendrocyte death or reduction of process length or complexity upon exposure to either Th17-conditioned medium or $\text{TNF-}\alpha$ and $\text{IFN-}\gamma$ over a period of 12 to 48 h. However, our in vivo data show long-lasting engagement resulting in a close proximity between T cells and oligodendrocytes for >70 min; local soluble factors secreted by Th17 cells could reach high concentrations in the microenvironment during such stable time periods. Most interestingly, we found that CD29, an

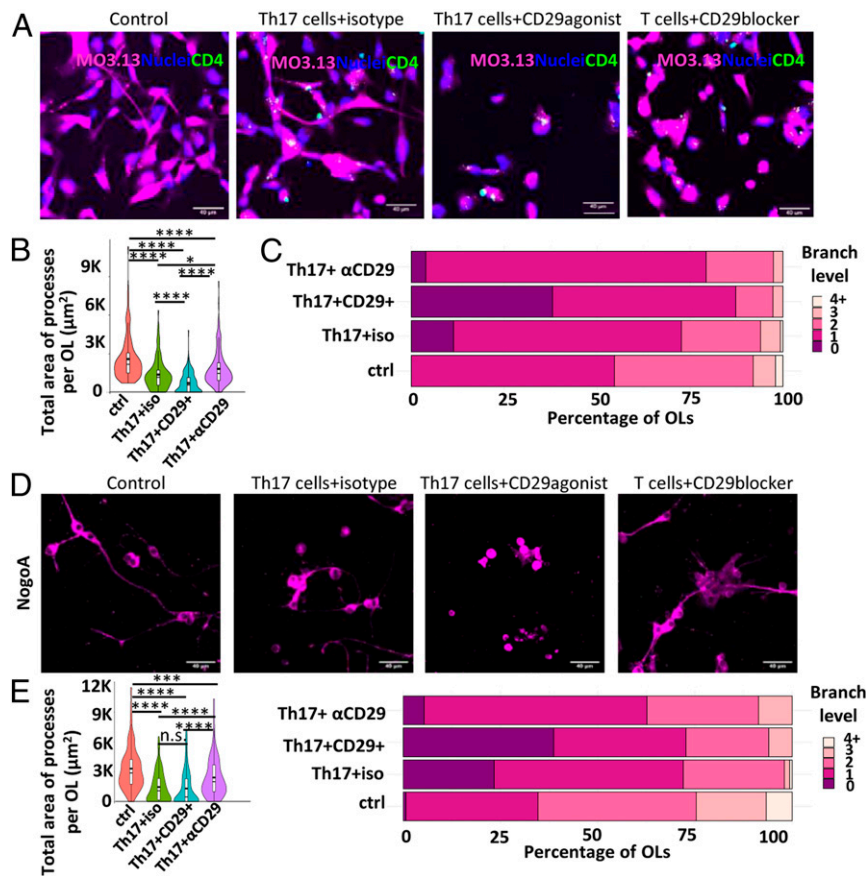


Fig. 7. Blocking CD29 on T cells protects oligodendrocytes from Th17 cell-mediated injury. (A–C) Impact of Th17 pretreatment by CD29 agonist or antagonist before coculture with human oligodendrocytic cell line MO3.13 cell in vitro. (A) Representative confocal microscopy images and (B and C) quantitative analysis of the total area of processes (Left) and branch level complexity of MO3.13 oligodendrocytic cells ($n = 3$ T cell donors and three different experiments, analysis of $n \geq 150$ MO3.13 cells/condition). (Scale bar, 40 μm .) (D–F) Impact of Th17 pretreatment with CD29 agonist or antagonist on human oligodendrocyte (OL) in vitro. (D) Representative confocal microscopy images and (E) quantitative analysis of the total area of processes (Left) and branch level complexity per OL ($n = 3$ T cell donors and $n = 2$ different OL preparations, $n \geq 150$ OLs/condition). (Scale bar, 40 μm .) Statistical analyses for B and D were performed using one-way ANOVA with Tukey's post hoc test. n.s.: not significant; * $P < 0.05$; *** $P < 0.001$; **** $P < 0.0001$.

integrin that triggers vesicular release of glutamate (37), is increased on murine and human Th17-polarized cells compared to Th2-polarized cells, as are molecules of the vesicular release pathways for glutamate. We, moreover, showed that Th17-polarized cells released higher levels of glutamate compared to Th2-polarized cells upon direct contact with oligodendrocytes, suggesting a potential for glutamate-mediated excitotoxicity to play a major role in the greater Th17-induced injury to oligodendrocyte processes compared to the more limited Th2-induced injury.

In line with Wosik et al. (70), we found human oligodendrocytes to be rather resistant to toxic factors, mimicking characteristics of the human CNS with its highly differentiated stable cell composition. Namely glutamate did not increase oligodendrocyte death. However, recent studies suggest that the oligodendrocyte functional state affects disease severity in MS (71). Here, scRNAseq analysis of human oligodendrocytes revealed that glutamate affected their expression of genes involved in the biosynthesis of cholesterol and lipids, including genes acting as negative regulators of cholesterol biosynthesis. Oligodendrocytic biosynthesis of cholesterol (46, 56) and lipids (55) has been shown to be essential for functional myelinating processes and myelin membrane growth (72). Notably, recently published RNA-sequencing data highlighted that cholesterol synthesis-related genes dominated as the top up-regulated pathways in oligodendrocytes during remyelination (46). Extending these findings, we here showed that, in parallel to an increased expression of

negative regulators of cholesterol biosynthesis, such as INSIG1, glutamate caused a dramatic reduction in the extension of human oligodendrocyte processes and in their ensheathing capacity as well as in the myelinated area in murine living brain slices. Notably, we observed up-regulation of SCD1 in mature oligodendrocytes exposed to glutamate, the inhibition of which promotes remyelination in organotypic slices following lysocleithin toxic injury (73). TMEM97, which is a target of lysocleithin and modulators to promote survival of neurons and oligodendrocytes following acute traumatic brain injury and in clinical trials for Alzheimer's disease (54), was also up-regulated. We therefore speculate that altered gene expression contributes to injury of human oligodendrocytes and to the observed impaired myelin ensheathing capacity in human and mice upon exposure to Th17-released glutamate. Some apoptosis-related genes were mildly up-regulated in stressed oligodendrocytes upon exposure to glutamate for 12 h, in line with our data showing that the impact of Th17 cells and of glutamate is first and most pronounced on oligodendrocyte processes at this early time point.

Our discovery goes along with reports on down-regulated expression of glutamate transporters EAAT-1 and EAAT-2 by oligodendrocytes in MS brain WM, preventing efficient removal and possibly contributing to increased extracellular glutamate levels and increased vulnerability to glutamate excitotoxicity in vivo (74). We have previously demonstrated the neuroprotective impact of restricting glutamate release by Th17 cells (37). This was

associated with a preservation of both myelin and myelinated axons. To disentangle the potential for protection of oligodendrocyte processes and myelin from the preservation of neuroaxonal processes and to parallel these findings in humans, we pretreated human Th17 cells with both CD29 agonist and antagonist before coculture with oligodendrocytes. Hereby, we uncovered a deleterious impact of CD29 activation on Th17-mediated toxicity toward human oligodendrocytes, while blocking CD29 on Th17 cells protected human oligodendrocyte processes, indicating direct damage to oligodendrocyte cell processes by human Th17 cells.

Finally, our data show that oligodendrocytes in direct contact with CD4⁺ T cells are significantly more likely to express cleaved caspase-3 than oligodendrocytes without CD4⁺ T cells in the vicinity in EAE. Oligodendrocytes in early MS lesions were previously shown to be immunoreactive for caspase-3 (75). Our data suggest that T cell-mediated oligodendrocyte stress plays a role in induction of oligodendrocyte injury in neuroinflammatory conditions. Furthermore, we could demonstrate that activated CD4⁺ T cells from MS subjects show a higher toxicity toward oligodendrocytes compared to CD4⁺ T cells from healthy controls, that contact with human Th17 cells is associated with increased cell death of human oligodendrocytes, and that CD4⁺ T cells and oligodendrocytes in direct juxtaposition are frequent in postmortem-derived CNS material of MS patients. Our data hence indicate detrimental function by direct T cell interactions with oligodendrocytes in human MS.

Altogether, our findings indicate that direct prolonged contacts between proinflammatory Th17 cells and oligodendrocytes contribute to oligodendrocyte injury in neuroinflammatory conditions such as MS and EAE. Our results further demonstrate that interaction with oligodendrocytes is contact dependent and significantly stronger in the proinflammatory Th17-polarized cell subset compared to their Th2-polarized counterpart and in activated CD4⁺ T cells from MS subjects compared to age- and sex-matched healthy controls. Finally, we showed that glutamate, which can be released from vesicles by Th17 cells in the local microenvironment following contact with oligodendrocytes and CD29 activation, can injure oligodendrocyte processes. Glutamate altered expression of genes implicated in cholesterol and lipid synthesis in oligodendrocytes and decreased myelination, but blocking CD29 preserved oligodendrocyte cell processes from Th17-mediated injury. We can therefore conclude that CD29-triggered glutamate release in close vicinity to the target cell contributes to Th17-mediated worsening of demyelination (24) and oligodendrocyte injury in MS and EAE. The relevance of such mechanisms in vivo is difficult to specifically ascertain, since CD29 blocking abrogates the capacity of CD4⁺ T cells to infiltrate the CNS and therapeutic administration of anti-CD29 antibody Hmb1-1 induced an infusion reaction in EAE mice. Nevertheless, our data on human oligodendrocytes and human Th17 cells suggest the potential for a therapeutic intervention in MS targeting CD29. In fact, we have recently demonstrated that interfering with the CD29-triggered glutamate release cascade in Th17 cells improves EAE (37). Future clinical developmental studies should address specific modifications of CD29 without systemic neutralization to limit side effects on physiological functions of CD29.

In conclusion, we provide intravital and human evidence for direct detrimental attack of proinflammatory CD29-expressing and glutamate-releasing Th17 cells against the myelin compartment, supporting targeted therapeutic strategies to reduce accumulation of neuroglial dysfunction and clinical deficits in MS.

Materials and Methods

Mice. B6.GFP, B6.CFP, B6.2D2.GFP, and B6.2D2.CFP mice (76, 77) were used to isolate T cells. Antigen-presenting cells were isolated from C57BL/6 mice (Janvier Labs). C57BL/6.CNP.Cre × C57BL/6.loxp.ROSA.tdRFP mice (78) and Rag2^{-/-}cgn^{-/-} mice (79) were used as recipients for EAE induction. All animal

experiments were approved by local authorities and performed in accordance with German Animal Protection Laws.

Passive EAE. Donor mice were immunized subcutaneously with 200 µg MOG₃₅₋₅₅ in 100 µL complete Freund's adjuvant (CFA) emulsion and 400 ng pertussis toxin (PTX) intraperitoneally. T cells were collected from spleen and lymph nodes and reactivated in vitro with MOG₃₅₋₅₅ in the presence of IL-23 and IFN-γ. A total of 2.5 to 5 × 10⁶ MOG-specific activated T cells were intravenously transferred into recipient mice, and non-Rag2^{-/-}cgn^{-/-} mice were treated additionally with PTX.

Active EAE. C57BL/6 mice were immunized subcutaneously with 200 µg MOG₃₅₋₅₅ in 200 µL CFA emulsion. Additionally, C57BL/6 mice received 200 ng PTX (Hooke kit, Hooke Laboratories) intraperitoneally at the time of immunization and 24 h later.

EAE Scoring. Mice were scored for clinical symptoms daily, and signs of classical (active) EAE were translated into clinical scores ranging from 0 to 5 (*SI Appendix, Supplemental Extended Methods*).

MOG-Specific and Polyclonal Murine Th17 Cell and Th2 Culture. Single cells were isolated from spleen and lymph nodes before magnetic bead-based cell sorting. CD4⁺CD62L^{hi} cells were stimulated with 2 µg/mL α-CD3 (BD Bioscience) in the presence of irradiated CD90⁺ cell-depleted C57BL/6 splenocytes. Naïve T cells were cultured differentiated into effector cells using different cytokine compositions (*SI Appendix, Supplemental Extended Methods*).

Intravital Two-Photon Imaging and Analysis. Operation procedures and two-photon laser scanning microscopy were performed as described previously (27, 80). In brief, mice were anesthetized, and imaging was performed following brain stem window surgery. Noise reduction was achieved by the software's "medium filter." After automatic drift correction, T cell tracks were created using the tracking tool implemented in Imaris software and manually corrected. Only T cells with a track duration of more than 10 min were used for contact analysis, which was performed manually. Meandering index (track displacement/track length), arrest coefficient (percentage of time points with speed ≤ 2 µm/min) (81), and mean speed were analyzed for each cell tracked.

Immunostaining of CNS Tissue.

Mouse. Frozen sagittal cryotome sections of EAE mouse brains and spinal cords were thawed, permeabilized, blocked with normal goat serum, stained with primary antibodies followed by secondary antibodies and nuclear counterstaining with DAPI dihydrochloride (Sigma-Aldrich Corp.). Afterward, slides were coverslipped using ProLong Gold Antifade Mountant (Thermo Fisher Scientific Inc.).

Human. All human CNS material was processed and stored at the Centre de Recherche du Centre Hospitalier de l'Université de Montréal (CRCHUM) with full ethical approval (BH07.001). Autopsy samples were preserved and lesions classified using luxol fast blue/haematoxylin & eosin staining and Oil Red O staining as previously published (82, 83). Frozen sections of CNS autopsy specimens were obtained from a total of five MS patients (*SI Appendix, Table S2*). Sections were fixed in paraformaldehyde 3%, blocked with 10% species-specific serum and then incubated at 4 °C with primary antibodies (*SI Appendix, Table S3*) followed by secondary antibodies and DAPI.

For further information on antibodies and staining procedures, reference *SI Appendix, Supplemental Extended Methods*.

Human T Cell Isolation and Culture. Written informed consent was obtained from every donor prior to sample collection (CRCHUM ethic committee approval Nos. SL05.022, SL05.023, and BH07.001). Peripheral blood was obtained by venous puncture of healthy subjects, and memory CD4⁺ T cells were magnetically isolated from peripheral blood mononuclear cells (PBMCs) following gradient centrifugation as previously published (14, 84). T cells were cultured and skewed into effector Th2 cells or Th17 cells as previously published (14). For further information, see also *SI Appendix, Supplemental Extended Methods*. For studies comparing CD4⁺ T cells from MS subjects with healthy controls, frozen PBMCs from untreated MS and age- and sex-matched healthy controls were gently thawed in fetal bovine serum (FBS). CD4⁺ T cells were magnetically isolated and then rested for 2 h in the incubator before activation on plate-bound anti-CD3 (0.5 µg/mL) and soluble anti-CD28 (0.5 µg/mL) without additional cytokine. For cytospin, cells were processed as previously published (14).

Human Oligodendrocyte/T Cell Coculture. Human adult oligodendrocytes in primary culture were generated by the group of J.A. using fresh brain tissue samples as described in *SI Appendix, Supplemental Extended Methods*. For MO3.13, human oligodendrocytic cells were used at P3 to P6 and prepared as previously published (14) and as described in *SI Appendix, Supplemental Extended Methods*. For the ensheathing assay, human adult oligodendrocytes were plated on nanofiber-coated microplates and cultured for 4 d before treatment with glutamate for indicated concentrations in duplicates. Glutamate was added every 2 d for 14 d. For the CD29 assay, human Th17 cells were preincubated with either isotype, anti-CD29 (P5D2, R&D), or CD29 agonist (TS2/16, BioLegend) at 10 $\mu\text{g}/\text{mL}$ for 1 h. Cells were then washed and resuspended in fresh X-vivo medium before addition to either the MO3.13 human oligodendrocytic cell line or human oligodendrocytes in primary culture as described for 12 h of coculture. Glutamate levels in the supernatants were determined using the glutamate assay kit (MAK004-1KT, Merck) according to the manufacturer's instructions.

Organotypic Hippocampal Slice Cultures. Organotypic hippocampal slice cultures (OHSCs) were prepared and cultured following the methods established by Stoppini et al. (85) and the protocol described by Gogolla et al. (86). For the analysis of the effect of T cells on myelin, OHSCs were preincubated until 10DIV (days in vitro), followed by a demyelinating treatment with 0.5 mg/mL LPC for 17 h. After 12DIV, OHSCs were cocultured with Th17- or Th2-skewed CD4⁺ cells for 72 h, after which the culture medium was changed and the slice cultures were further incubated for five more days. For further information on fixation and staining procedures reference *SI Appendix, Supplemental Extended Methods*. For the analysis of glutamate toxicity, OHSCs were treated on days 15 to 17 of culture with 1 mM glutamate for 24 h. For interaction analysis, OHSCs were treated with 0.2×10^6 T cells per slice. After 24 to 48 h of coculture, two-photon imaging was performed to visualize interactions.

scRNAseq. Two different preparations of adult human oligodendrocytes in primary culture were exposed to vehicle or glutamate 1 mM for 12 h.

scRNAseq libraries were created using 10x Chromium version 2.0 and sequenced with the Illumina NovaSeq6000 SP PE150 at the McGill University and Genome Québec Innovation Centre. scRNAseq was performed using a droplet sequencing approach (10x Chromium). Data demultiplexing and genome mapping were performed with the cell ranger analysis pipeline (87). Reads were aligned to reference genome GRCh38. For further information on parameters of analysis and quality assurance, see also *SI Appendix, Supplemental Extended Methods*. Genes were considered to be significantly differentially expressed (DEGs) between groups if they had an adjusted *P* value < 0.01 and an absolute LFC ≥ 0.3 . The gene set enrichment analysis was first done using a Fisher test onto the Gene Ontology Biological Processes 2018 annotation.

Statistical Analysis. All data were analyzed using GraphPad Prism 6 (GraphPad Software) or R (88) using the ggplot2 package (89). After assessing for distribution and when appropriate, mean group differences were investigated by one-way ANOVA followed by Tukey's multiple comparison test, Mann-Whitney *U* test, or independent-sample two-tailed *t* tests or, when indicated, paired *t* test. The significance level was set at 0.05.

More detailed information on material and methods is given in *SI Appendix, Supplemental Extended Methods*.

Data Availability. RNAseq data have been deposited in Gene Expression Omnibus (GSE180670) (44).

ACKNOWLEDGMENTS. We thank Christin Liefänder, Silke Fregin, Audrey Daigneault, and Heike Ehrengard for excellent technical assistance and Rosalind Morley and Cheryl Ernest for proofreading the manuscript. This study was supported by the Deutsche Forschungsgemeinschaft (Collaborative Research Center SFB/CRC-TR-128 to F.Z. and S.B., SFB 1080 and SFB 1292 to F.Z.), the Gemeinnützige Hertie-Stiftung (mylab 2017 to S.B.), the Canadian Institutes of Health Research (162430 to C.L.), and the Multiple Sclerosis Society of Canada (MS Society Grant ID [EGID] 3322 to C.L. and studentship to H.J.). C.L. holds a Junior Scholar Award from the Fonds de recherche du Québec-Santé.

- R. Dutta, B. D. Trapp, Mechanisms of neuronal dysfunction and degeneration in multiple sclerosis. *Prog. Neurobiol.* **93**, 1–12 (2011).
- C. Laroche, T. Uphaus, A. Prat, F. Zipp, Secondary progression in multiple sclerosis: Neuronal exhaustion or distinct pathology? *Trends Neurosci.* **39**, 325–339 (2016).
- D. H. Mahad, B. D. Trapp, H. Lassmann, Pathological mechanisms in progressive multiple sclerosis. *Lancet Neurol.* **14**, 183–193 (2015).
- K.-A. Nave, Myelination and the trophic support of long axons. *Nat. Rev. Neurosci.* **11**, 275–283 (2010).
- R. J. M. Franklin, C. French-Constant, J. M. Edgar, K. J. Smith, Neuroprotection and repair in multiple sclerosis. *Nat. Rev. Neurol.* **8**, 624–634 (2012).
- B. D. Trapp, K.-A. Nave, Multiple sclerosis: An immune or neurodegenerative disorder? *Annu. Rev. Neurosci.* **31**, 247–269 (2008).
- S. W. Way et al., Pharmaceutical integrated stress response enhancement protects oligodendrocytes and provides a potential multiple sclerosis therapeutic. *Nat. Commun.* **6**, 6532 (2015).
- Q. L. Cui et al., Sublethal oligodendrocyte injury: A reversible condition in multiple sclerosis? *Ann. Neurol.* **81**, 811–824 (2017).
- C. A. Dendrou, L. Fugger, M. A. Friese, Immunopathology of multiple sclerosis. *Nat. Rev. Immunol.* **15**, 545–558 (2015).
- M. A. Friese, B. Schattling, L. Fugger, Mechanisms of neurodegeneration and axonal dysfunction in multiple sclerosis. *Nat. Rev. Neurol.* **10**, 225–238 (2014).
- J. Goverman, Autoimmune T cell responses in the central nervous system. *Nat. Rev. Immunol.* **9**, 393–407 (2009).
- L. Codarri et al., ROR γ t drives production of the cytokine GM-CSF in helper T cells, which is essential for the effector phase of autoimmune neuroinflammation. *Nat. Immunol.* **12**, 560–567 (2011).
- D. W. Luchtman, E. Ellwardt, C. Laroche, F. Zipp, IL-17 and related cytokines involved in the pathology and immunotherapy of multiple sclerosis: Current and future developments. *Cytokine Growth Factor Rev.* **25**, 403–413 (2014).
- C. Laroche et al., Melanoma cell adhesion molecule identifies encephalitogenic T lymphocytes and promotes their recruitment to the central nervous system. *Brain* **135**, 2906–2924 (2012).
- H. Kebir et al., Preferential recruitment of interferon- γ -expressing TH17 cells in multiple sclerosis. *Ann. Neurol.* **66**, 390–402 (2009).
- P. J. Darlington et al., Canadian MS/BMT Study Group, Diminished Th17 (not Th1) responses underlie multiple sclerosis disease abrogation after hematopoietic stem cell transplantation. *Ann. Neurol.* **73**, 341–354 (2013).
- J. van Langelaar et al., T helper 17 cells associate with multiple sclerosis disease activity: Perspectives for early intervention. *Brain* **141**, 1334–1349 (2018).
- E. Havrdová et al., Activity of secukinumab, an anti-IL-17A antibody, on brain lesions in RRMS: Results from a randomized, proof-of-concept study. *J. Neurology.* **263**, 1287–1295 (2016).
- H. Kebir et al., Human TH17 lymphocytes promote blood-brain barrier disruption and central nervous system inflammation. *Nat. Med.* **13**, 1173–1175 (2007).
- C. Laroche, J. I. Alvarez, A. Prat, How do immune cells overcome the blood-brain barrier in multiple sclerosis? *FEBS Lett.* **585**, 3770–3780 (2011).
- J. P. Antel, K. Williams, M. Blain, E. McRea, J. McLaurin, Oligodendrocyte lysis by CD4⁺ T cells independent of tumor necrosis factor. *Ann. Neurol.* **35**, 341–348 (1994).
- A. L. Hestvik, G. Skorstad, F. Vartdal, T. Holmøy, Idiotope-specific CD4⁺ T cells induce apoptosis of human oligodendrocytes. *J. Autoimmun.* **32**, 125–132 (2009).
- F. Zaguia et al., Cytotoxic NKG2C⁺ CD4 T cells target oligodendrocytes in multiple sclerosis. *J. Immunol.* **190**, 2510–2518 (2013).
- E. G. Baxi et al., Transfer of myelin-reactive th17 cells impairs endogenous remyelination in the central nervous system of cuprizone-fed mice. *J. Neurosci.* **35**, 8626–8639 (2015).
- J. P. Antel, E. McRea, U. Ladiwala, Y. F. Qin, B. Becher, Non-MHC-restricted cell-mediated lysis of human oligodendrocytes in vitro: Relation with CD56 expression. *J. Immunol.* **160**, 1606–1611 (1998).
- V. Siffrin et al., FRET based ratiometric Ca²⁺ imaging to investigate immune-mediated neuronal and axonal damage processes in experimental autoimmune encephalomyelitis. *J. Neurosci. Methods* **249**, 8–15 (2015).
- V. Siffrin et al., In vivo imaging of partially reversible th17 cell-induced neuronal dysfunction in the course of encephalomyelitis. *Immunity* **33**, 424–436 (2010).
- M. J. Miller, O. Safrina, I. Parker, M. D. Cahalan, Imaging the single cell dynamics of CD4⁺ T cell activation by dendritic cells in lymph nodes. *J. Exp. Med.* **200**, 847–856 (2004).
- C. Schläger et al., Effector T-cell trafficking between the leptomeninges and the cerebrospinal fluid. *Nature* **530**, 349–353 (2016).
- A. M. Falcão et al., Disease-specific oligodendrocyte lineage cells arise in multiple sclerosis. *Nat. Med.* **24**, 1837–1844 (2018).
- J. M. Redwine, M. J. Buchmeier, C. F. Evans, In vivo expression of major histocompatibility complex molecules on oligodendrocytes and neurons during viral infection. *Am. J. Pathol.* **159**, 1219–1224 (2001).
- S. C. Lee, C. S. Raine, Multiple sclerosis: Oligodendrocytes in active lesions do not express class II major histocompatibility complex molecules. *J. Neuroimmunol.* **25**, 261–266 (1989).
- H. G. Lee et al., Pathogenic function of bystander-activated memory-like CD4⁺ T cells in autoimmune encephalomyelitis. *Nat. Commun.* **10**, 709 (2019).
- C. F. Vogelaar et al., Fast direct neuronal signaling via the IL-4 receptor as therapeutic target in neuroinflammation. *Sci. Transl. Med.* **10**, eaao2304 (2018).
- J. T. Walsh et al., MHCII-independent CD4⁺ T cells protect injured CNS neurons via IL-4. *J. Clin. Invest.* **125**, 699–714 (2015).
- A. Jäger, V. Dardalhon, R. A. Sobel, E. Bettelli, V. K. Kuchroo, Th1, Th17, and Th9 effector cells induce experimental autoimmune encephalomyelitis with different pathological phenotypes. *J. Immunol.* **183**, 7169–7177 (2009).
- K. Birkner et al., β 1-Integrin- and KV1.3 channel-dependent signaling stimulates glutamate release from Th17 cells. *J. Clin. Invest.* **130**, 715–732 (2020).

38. J. D. Clements, R. A. Lester, G. Tong, C. E. Jahr, G. L. Westbrook, The time course of glutamate in the synaptic cleft. *Science* **258**, 1498–1501 (1992).
39. A. Chang, A. Nishiyama, J. Peterson, J. Prineas, B. D. Trapp, NG2-positive oligodendrocyte progenitor cells in adult human brain and multiple sclerosis lesions. *J. Neurosci.* **20**, 6404–6412 (2000).
40. A. Polito, R. Reynolds, NG2-expressing cells as oligodendrocyte progenitors in the normal and demyelinated adult central nervous system. *J. Anat.* **207**, 707–716 (2005).
41. A. Nirwane, Y. Yao, Laminins and their receptors in the CNS. *Biol. Rev. Camb. Philos. Soc.*, 10.1111/brv.12454 (2018).
42. C. Esmonde-White *et al.*, Distinct Function-Related Molecular Profile of Adult Human A2B5-Positive Pre-Oligodendrocytes Versus Mature Oligodendrocytes. *J. Neuropathol. Exp. Neurol.* **78**, 468–479 (2019).
43. K. Perlman *et al.*, Developmental trajectory of oligodendrocyte progenitor cells in the human brain revealed by single cell RNA sequencing. *Glia* **68**, 1291–1303 (2020).
44. C. Larochele, H. Jamann, O. Tastet, Q. Cui, J. Antel, scRNAseq of human oligodendrocytes in primary culture exposed to glutamate vs. vehicle. NCBI GEO (National Center for Biotechnology Information *Gene Expression Omnibus*). <http://www.ncbi.nlm.nih.gov/geo/query/acc.cgi?acc=GSE180670>. Deposited 22 July 2021.
45. T. Ilicic *et al.*, Classification of low quality cells from single-cell RNA-seq data. *Genome Biol.* **17**, 29 (2016).
46. R. R. Voskuhl *et al.*, Gene expression in oligodendrocytes during remyelination reveals cholesterol homeostasis as a therapeutic target in multiple sclerosis. *Proc. Natl. Acad. Sci. U.S.A.* **116**, 10130–10139 (2019).
47. E. S. Mathews *et al.*, Mutation of 3-hydroxy-3-methylglutaryl CoA synthase I reveals requirements for isoprenoid and cholesterol synthesis in oligodendrocyte migration arrest, axon wrapping, and myelin gene expression. *J. Neurosci.* **34**, 3402–3412 (2014).
48. T. Yang *et al.*, Crucial step in cholesterol homeostasis: Sterols promote binding of SCAP to INSIG-1, a membrane protein that facilitates retention of SREBPs in ER. *Cell* **110**, 489–500 (2002).
49. Y. Sun *et al.*, Stearoyl-CoA desaturase inhibits ATP-binding cassette transporter A1-mediated cholesterol efflux and modulates membrane domain structure. *J. Biol. Chem.* **278**, 5813–5820 (2003).
50. C. M. Paton, J. M. Ntambi, Loss of stearoyl-CoA desaturase activity leads to free cholesterol synthesis through increased Xbp-1 splicing. *Am. J. Physiol. Endocrinol. Metab.* **299**, E1066–E1075 (2010).
51. C. M. Paton, J. M. Ntambi, Biochemical and physiological function of stearoyl-CoA desaturase. *Am. J. Physiol. Endocrinol. Metab.* **297**, E28–E37 (2009).
52. D. Ebrahimi-Fakhari *et al.*, Reduction of TMEM97 increases NPC1 protein levels and restores cholesterol trafficking in Niemann-pick type C1 disease cells. *Hum. Mol. Genet.* **25**, 3588–3599 (2016).
53. E. Vázquez-Rosa *et al.*, Neuroprotective efficacy of a sigma 2 receptor/TMEM97 modulator (DKR-1677) after traumatic brain injury. *ACS Chem. Neurosci.* **10**, 1595–1602 (2019).
54. M. Grundman *et al.*, A phase 1 clinical trial of the sigma-2 receptor complex allosteric antagonist CT1812, a novel therapeutic candidate for Alzheimer's disease. *Alzheimers Dement. (N. Y.)* **5**, 20–26 (2019).
55. H. Rolyan *et al.*, Defects of lipid synthesis are linked to the age-dependent demyelination caused by lamin B1 overexpression. *J. Neurosci.* **35**, 12002–12017 (2015).
56. J. Gonzalez Cardona *et al.*, Quetiapine has an additive effect to triiodothyronine in inducing differentiation of oligodendrocyte precursor cells through induction of cholesterol biosynthesis. *PLoS One* **14**, e0221747 (2019).
57. M. Bauer *et al.*, Beta1 integrins differentially control extravasation of inflammatory cell subsets into the CNS during autoimmunity. *Proc. Natl. Acad. Sci. U.S.A.* **106**, 1920–1925 (2009).
58. K. Iwata *et al.*, The human oligodendrocyte proteome. *Proteomics* **13**, 3548–3553 (2013).
59. N. Kawakami *et al.*, The activation status of neuroantigen-specific T cells in the target organ determines the clinical outcome of autoimmune encephalomyelitis. *J. Exp. Med.* **199**, 185–197 (2004).
60. E. J. McMahon, S. L. Bailey, C. V. Castenada, H. Waldner, S. D. Miller, Epitope spreading initiates in the CNS in two mouse models of multiple sclerosis. *Nat. Med.* **11**, 335–339 (2005).
61. S. M. Tompkins *et al.*, De novo central nervous system processing of myelin antigen is required for the initiation of experimental autoimmune encephalomyelitis. *J. Immunol.* **168**, 4173–4183 (2002).
62. M. Pesic *et al.*, 2-photon imaging of phagocyte-mediated T cell activation in the CNS. *J. Clin. Invest.* **123**, 1192–1201 (2013).
63. M. Mittelbrunn *et al.*, Imaging of plasmacytoid dendritic cell interactions with T cells. *Blood* **113**, 75–84 (2009).
64. T. Worbs, T. R. Mempel, J. Bölter, U. H. von Andrian, R. Förster, CCR7 ligands stimulate the intranodal motility of T lymphocytes in vivo. *J. Exp. Med.* **204**, 489–495 (2007).
65. R. T. Boscacci *et al.*, Comprehensive analysis of lymph node stroma-expressed Ig superfamily members reveals redundant and nonredundant roles for ICAM-1, ICAM-2, and VCAM-1 in lymphocyte homing. *Blood* **116**, 915–925 (2010).
66. J. Satoh, S. U. Kim, L. F. Kastrukoff, F. Takei, Expression and induction of intercellular adhesion molecules (ICAMs) and major histocompatibility complex (MHC) antigens on cultured murine oligodendrocytes and astrocytes. *J. Neurosci. Res.* **29**, 1–12 (1991).
67. C. S. Moore *et al.*, Direct and indirect effects of immune and central nervous system-resident cells on human oligodendrocyte progenitor cell differentiation. *J. Immunol.* **194**, 761–772 (2015).
68. E. R. Pierson, J. M. Goverman, GM-CSF is not essential for experimental autoimmune encephalomyelitis but promotes brain-targeted disease. *JCI Insight* **2**, e92362 (2017).
69. S. Haak *et al.*, IL-17A and IL-17F do not contribute vitally to autoimmune neuroinflammation in mice. *J. Clin. Invest.* **119**, 61–69 (2009).
70. K. Wosik *et al.*, Resistance of human adult oligodendrocytes to AMPA/kainate receptor-mediated glutamate injury. *Brain* **127**, 2636–2648 (2004).
71. S. Jäkel *et al.*, Altered human oligodendrocyte heterogeneity in multiple sclerosis. *Nature* **566**, 543–547 (2019).
72. G. Saher *et al.*, High cholesterol level is essential for myelin membrane growth. *Nat. Neurosci.* **8**, 468–475 (2005).
73. J. F. J. Bogie *et al.*, Stearoyl-CoA desaturase-1 impairs the reparative properties of macrophages and microglia in the brain. *J. Exp. Med.* **217**, e20191660 (2020).
74. D. Pitt, I. E. Nagelmeier, H. C. Wilson, C. S. Raine, Glutamate uptake by oligodendrocytes: Implications for excitotoxicity in multiple sclerosis. *Neurology* **61**, 1113–1120 (2003).
75. J. W. Prineas, J. D. E. Parratt, Oligodendrocytes and the early multiple sclerosis lesion. *Ann. Neurol.* **72**, 18–31 (2012).
76. A. K. Hadjantonakis, S. Macmaster, A. Nagy, Embryonic stem cells and mice expressing different GFP variants for multiple non-invasive reporter usage within a single animal. *BMC Biotechnol.* **2**, 11 (2002).
77. E. Bettelli *et al.*, Myelin oligodendrocyte glycoprotein-specific T cell receptor transgenic mice develop spontaneous autoimmune optic neuritis. *J. Exp. Med.* **197**, 1073–1081 (2003).
78. H. Luche, O. Weber, T. Nageswara Rao, C. Blum, H. J. Fehling, Faithful activation of an extra-bright red fluorescent protein in “knock-in” Cre-reporter mice ideally suited for lineage tracing studies. *Eur. J. Immunol.* **37**, 43–53 (2007).
79. F. Mazurier *et al.*, A novel immunodeficient mouse model—RAG2 x common cytokine receptor gamma chain double mutants—Requiring exogenous cytokine administration for human hematopoietic stem cell engraftment. *J. Interferon Cytokine Res.* **19**, 533–541 (1999).
80. J. Herz *et al.*, Expanding two-photon intravital microscopy to the infrared by means of optical parametric oscillator. *Biophys. J.* **98**, 715–723 (2010).
81. J. Herz, K. R. Johnson, D. B. McGavern, Therapeutic antiviral T cells noncytopathically clear persistently infected microglia after conversion into antigen-presenting cells. *J. Exp. Med.* **212**, 1153–1169 (2015).
82. T. Dhaeze *et al.*, CD70 defines a subset of proinflammatory and CNS-pathogenic T_H17/T_H17 lymphocytes and is overexpressed in multiple sclerosis. *Cell. Mol. Immunol.* **16**, 652–665 (2019).
83. T. Kuhlmann *et al.*, An updated histological classification system for multiple sclerosis lesions. *Acta Neuropathol.* **133**, 13–24 (2017).
84. C. Larochele *et al.*, Melanoma cell adhesion molecule-positive CD8 T lymphocytes mediate central nervous system inflammation. *Ann. Neurol.* **78**, 39–53 (2015).
85. L. Stoppini, P. A. Buchs, D. Müller, A simple method for organotypic cultures of nervous tissue. *J. Neurosci. Methods* **37**, 173–182 (1991).
86. N. Gogolla, I. Galimberti, V. DePaola, P. Caroni, Preparation of organotypic hippocampal slice cultures for long-term live imaging. *Nat. Protoc.* **1**, 1165–1171 (2006).
87. Genomics Single Cell 3' Gene Expression and VDJ Assembly, cell ranger 3.0.2. <https://github.com/10XGenomics/cellranger>. Accessed 31 May 2021.
88. R Core Team, R: A Language and Environment for Statistical Computing (R Foundation for Statistical Computing, Vienna, Austria, 2013). <https://www.R-project.org/>. Accessed 31 May 2021.
89. H. Wickham, ggplot2: Elegant Graphics for Data Analysis (Springer-Verlag, New York, 2016). <https://ggplot2.tidyverse.org>. Accessed 31 May 2021.